Available online at www.sciencedirect.com

ScienceDirect

journal homepage: www.elsevier.com/locate/he

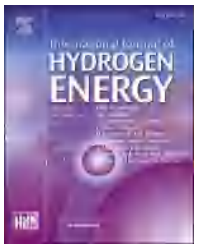

Study on LiI and KI with low melting temperature for electrolyte replenishment in molten carbonate fuel cells

Jae Kwan Bae [a,b], *Hyun-Woo Kim* [a,b], *Grazia Accardo* [a], *Ghun Sik Kim* [a,b], *Hyung Chul Ham* [a], *Seong-Cheol Jang* [a], *Yong Soo Cho* [b,**], *Sung Pil Yoon* [a,*]

[a] *Center for Hydrogen and Fuel Cell Research, Korea Institute of Science and Technology, Seoul 02792, South Korea*
[b] *Department of Materials Science and Engineering, Yonsei University, Seoul 03722, South Korea*

HIGHLIGHTS

- Electrolyte precursors (LiI and KI) were selected by thermodynamic calculation.
- LiI and KI with low melting temp. are suitable for electrolyte replenishment.
- LiI and KI supplements are effective in ensuring stable performance for MCFCs.

ARTICLE INFO

Article history:
Received 18 June 2019
Received in revised form
5 August 2019
Accepted 8 August 2019
Available online 9 September 2019

Keywords:
Electrolyte precursor
In-situ
KI
LiI
MCFC
Replenishment

ABSTRACT

Molten carbonate fuel cells (MCFCs) are regarded as the closest fuel cell to commercialization due to their high capacity and energy efficiency. However, they are operated at a high temperature (620 °C or higher), where liquid electrolyte loss occurs during operation; hence, their lifetime is limited. For the long-term operation of MCFCs, it is essential to develop a novel method to replenish the electrolyte during operation. However, it is very difficult to directly inject the electrolyte, $(Li_{0.62}K_{0.38})_2CO_3$, into each unit cell of the stack unless it is supplemented through liquid or gas phase at low temperature. It was verified whether LiI and KI, which have low melting points and high vapor pressures, could replenish the lost electrolyte in MCFCs. In this study, the LiI and KI injected into the unit cell in liquid phase showed a similar tendency to the Li/K carbonate electrolyte. This is because LiI and KI react with the CO_2/O_2 gases supplied to the cathode during MCFC operation to form Li/K carbonate electrolytes.

Introduction

Molten carbonate fuel cells (MCFCs) are an interesting type of high-temperature fuel cells [1–6] due to the use of liquid carbonate as the electrolyte. Unlike other types of fuel cells, MCFCs can utilize not only hydrogen but also natural gas, syngas, and liquid propane gas (LPG) as fuel. The cells could be particularly useful as decentralized power generators or emergency power generators since power can easily be

* *Corresponding author.*
** *Corresponding author.*
E-mail addresses: ycho@yonsei.ac.kr (Y.S. Cho), spyoon@kist.re.kr (S.P. Yoon).
https://doi.org/10.1016/j.ijhydene.2019.08.050

supplied from the units using existing liquid natural gas (LNG) pipelines. Because of such advantages [7–10], MCFCs currently produce more than 300 MW of electricity worldwide, however, a lifetime of these systems can be affected by several drawbacks [11–13] as the loss of electrolytes or other elements during long-term operation [14–17]. There are two major mechanisms that lead to this loss as reported in Fig. 1. First, the mechanism involves with the loss from the lithiation of the NiO electrode during pre-treatment and corrosion of the metal-based cell frame wet seal area [18–21], and the second, depletion occurs through the volatilization of the electrolyte as hydroxide forms in the anode atmosphere [22,23].

In degradation phase 1, both the polarization resistance of the electrode and ohmic resistance increase due to the consumption of the electrolyte at the electrodes, and then the performance is gradually reduced. If the electrolyte is continuously volatilized during long-term operation, especially at the matrix, a drastic decrease in performance occurs as in degradation phase 2.

The electrolyte loss from MCFCs causes an adverse effect on the long-term operation due to the changes in electrolytic motility and the physical properties. For instance, the main effect of loss of electrolyte is a decrease in ionic conductivity due to a scarcity of charge-carrying medium [25,26]. Deficiency of electrolyte, therefore, roots a gradual decrease in cell voltage during operation, which almost exclusively occurs through the increase of internal resistance (IR).

Another effect of electrolyte loss is the formation of catastrophic cracks in the matrix, with an additional reduction of cell performances. In fact, electrolyte loss can lead to microfractures in the matrices; such hot spots, in turn, can lead to imperfections in the sealing of the fuel gas and oxidant gas, causing further corrosions and finally cracking the unit cell. In order to improve the long-term operation of MCFCs two strategies are proposed in the literature: employing additional electrolytes to compensate the loss [22] or inserting a eutectic composition of the electrolyte as powders during operation [14,24]. In previous studies, lab scale unit cells were operated up to 40,000 h through replenishing electrolyte or pre-overloaded electrolyte precursor.

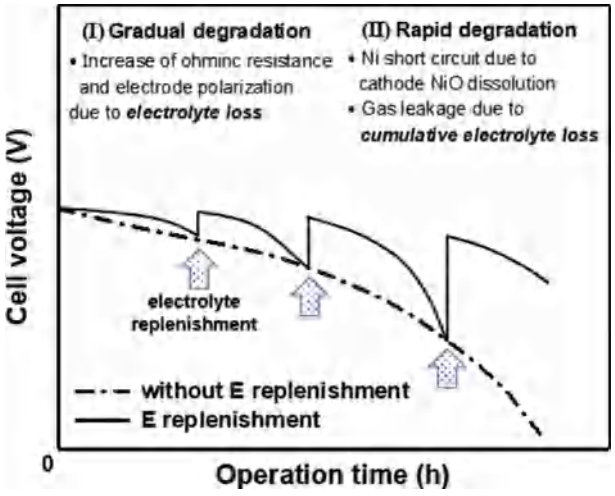

Fig. 1 – The mechanism by which MCFCs degrade and the qualitative effects of electrolyte replenishment to a cell [14,24].

These approaches achieved good results in the case of a single cell test but their application cannot be practically applied on a large scale MCFC stack system. In fact, it is very difficult to directly inject $(Li_{0.62}K_{0.38})_2CO_3$ having a eutectic point of higher than 500 °C into the stack, so that in order to improve the workability of the electrolyte replenishment, it is preferable to use an electrolyte precursor with a low melting point of below 300 °C. In this paper, various electrolyte precursor (EP) have been investigated as candidates for direct injection in MCFC systems. The electrolyte precursors were suitable to react with CO_2/O_2 to produce $(Li_{0.62}K_{0.38})_2CO_3$ due to their low melting point and high vapor pressure. As a result, the noticeable improvement in performance longevity was observed by the EP replenishment, with the solid experimental evidence in cell voltage and polarization resistance comparable to the standard $(Li_{0.62}K_{0.38})_2CO_3$ electrolyte.

Experimental

Electrolyte precursor (EP) selection

Suitable EPs were investigated using "STANJAN equilibrium solver" [27], the thermodynamic equilibrium calculation program. STANJAN calculates the chemical equilibrium state of products by minimizing the Gibbs free energy as a parameter of pressure and temperature, using a Lagrange multiplier. The required thermodynamic data were obtained from the JANAF table (https://janaf.nist.gov/). The reactivity of EP with carbon dioxide and oxygen was confirmed by thermogravimetric differential thermal analysis (TG/DTA) analysis (Q600, TA Instrument, US).

Cell set up

The unit cell, with a planar circle area of 6.606 cm^2 was fabricated using standard NiO cathode, standard Ni anode, and γ-$LiAlO_2$ matrix. All components were produced by TWIN energy Co. Korea. The electrolyte green sheet (MTFC Co., Korea) consisted of a mixture of lithium carbonate (JUNSEI Co., Japan) and potassium carbonate (DAEJUNG Co., Korea) in the composition of $(Li_{0.70}K_{0.30})_2CO_3$. The unit cell designed for electrolyte replacement is shown in Fig. 2. A tube for supplying the electrolyte and EP to the unit cell during operation is added to the cell frame of the air electrode in order to mitigate the effects of electrolyte loss in the cell. The unit cells were operated at 650 °C and the gas utilization was 0.1 to accelerate an electrolyte depletion under harsh conditions [14,24]. The performance and impedance analysis were carried out using a Solartron 1260 with a frequency analyzer 1287 (frequency range: 10 kHz to 0.01 Hz). While in an open-circuit voltage (OCV) state, there is no nitrogen in the anode exhaust gas, so the amount of nitrogen cross-over (N_2 Cross-over) from the cathode was measured using gas chromatography (GC) (Agilent Technologies Co., USA).

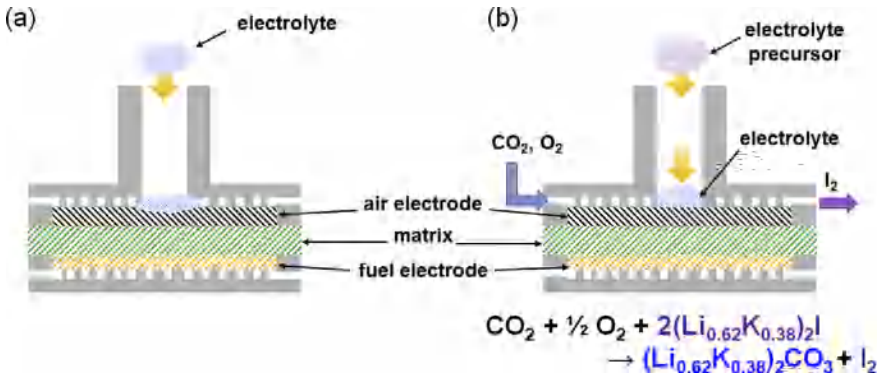

Fig. 2 – Schematic diagram of unit cells with injection tubes for a solid phase (a) electrolyte and (b) electrolyte precursor (EP).

Electrolyte addition

The electrolyte consisting of 62 mol% of lithium carbonate (Li_2CO_3) and 38 mol% of potassium carbonate (K_2CO_3) was initially melted at 650 °C and coagulated during cooling in a CO_2 atmosphere. The lithium potassium iodide compound was prepared by melting 62 mol% LiI and 38 mol% KI at 650 °C and coagulated in a reducing atmosphere. The melting points of coagulated $(L_{i0.62}K_{0.38})_2CO_3$) and $(Li_{0.62}K_{0.38})$I were measured by TG-DTA and were 497 °C and 298 °C, respectively.

Either coagulated electrolyte ($(L_{i0.62}K_{0.38})_2CO_3$) or coagulated EP ($(Li_{0.62}K_{0.38})$I) were injected at room temperature as a solid phase into a unit cell, which was specially designed as shown in Fig. 2. The injected $(L_{i0.62}K_{0.38})_2CO_3$ electrolyte powders were melted at the operating temperature of 650 °C and then the melts were penetrated directly into the electrode. On the other hand, in case of using the coagulated EP ($(Li_{0.62}K_{0.38})$I), the injected EP (melting point: 298 °C) powders were immediately melted at 650 °C and then CO_2/O_2 gases were flowed to the air electrode to induce conversion of the EP into $(L_{i0.62}K_{0.38})_2CO_3$ electrolyte.

Results and discussions

Thermodynamic results for electrolyte precursors in the air electrode atmosphere of an MCFC

According to the literature [28], a suitable EP has a low melting point and high vapor pressure and it can be transformed into the electrolyte in the air electrode atmosphere of an MCFC. Substances that satisfy these conditions include Li_2O and LiOH, and their hydrates, Li_3Sb_2, Li_3Bi, Li_2SO_4, $LiOC_2H_5$, $LiOCH_3$, LiI, LiBr, LiCl, LiF, Li_3N, $L_{i2}C_2$, $LiNH_2$, $LiMoO_4$, LiSn, $LiAlH_4$, LiPb, LiHg, and LiTi in lithium series. From the potassium series instead, K_2O, KOH and its hydrates, KBr, KCl, KF, K_3N, KNH_2, and K_2SO_4 were investigated. Of these candidates, LiI and KI were selected due to their properties and low costs. By using STANJAN to calculate the thermodynamic equilibrium of LiI and KI and their products, it was confirmed that the substances both transformed into electrolytes when injected into an MCFC air electrode as reported in Table 1.

Thermogravimetry & Differential Thermal Analysis (TG-DTA) was performed to confirm the reactivity of EPs (LiI, KI) under the MCFC operating condition. In the TG-DTA analysis, 20 mg of coagulated $(Li_{0.62}K_{0.38})$I was used and the temperature was increased from room temperature to 650 °C in a nitrogen atmosphere at a ramp rate of 10 °C/min. During heating the sample, the endothermic reaction was observed at 298 °C which is a melting point of the $(Li_{0.62}K_{0.38})$I (Fig. 3(a)). After reaching the target temperature of 650 °C, the isothermal operation was performed for 10 min to ensure the stabilization time. Consequently, it was confirmed that the initial mass of $(Li_{0.62}K_{0.38})$I was reduced by 10 wt% because of vaporization of surface hydrate and EP. After maintaining the sample at 650 °C, CO_2/O_2 gas was injected to induce reaction with EP. As shown in Fig. 3(b), the exothermic behaviour shows that the oxidation reaction of EP occurs at the time of introducing the oxidant gases. Fig. 3 (b) shows that the weight loss rate decreased after the rapid weight reduction because the carbonate liquid film produced by the oxidation reaction retards the diffusion of CO_2/O_2 needed to oxidize the remaining EP. No further mass changes were observed after 200 min of TG analysis with CO_2/O_2 gas injection. At this time, the mass change was reduced by 69.73% compared with the initial weight and 6.05 mg remained. The final weight was theoretically consistent with the weight of $(Li/K)_2CO_3$, which was produced by LiI and KI reacting with CO_2/O_2 to generate iodine vapor. This experiment proved that LiI and KI EPs were converted to the Li/K carbonate electrolyte under MCFC operating conditions.

Electrolyte replenishment into unit cells

Injection of excess electrolytes

After pre-treatment to remove any organic substances from the green sheet through an appropriate heat treatment in a CO_2 atmosphere, the cell was changed to the normal gas condition as shown in Table 2. After stabilization for 90 h, 0.05–0.06 g of electrolyte was injected at regular intervals. Table 3 summarizes the amount of electrolyte added via each injection.

Changes to the performance and impedance due to the electrolyte injection into the unit cell are shown in Fig. 4(a). The recovery of performance and IR was observed because the

Table 1 – Thermodynamic equilibrium calculation of electrolyte precursor in the air electrode atmosphere of MCFC at 923 K under 1 atm.

Reactant		Product	
Species	Equilibrium mol	Species	Equilibrium mol
LiI (*solid*)	2.24×10^{-3}	LiI (*gas*)	5.59×10^{-14}
		LiI (*liquid + solid*)	5.40×10^{-11}
		Li_2CO_3 (*liquid + solid*)	**1.12×10^{-3}**
		Li_2O (*solid*)	7.47×10^{-19}
		Li_2O_2 (*solid*)	1.29×10^{-21}
KI (*solid*)	1.37×10^{-3}	KI (*gas*)	1.10×10^{-10}
		KI (*liquid + solid*)	7.92×10^{-7}
		K_2CO_3 (*liquid + solid*)	**6.86×10^{-4}**
		K_2O (*solid*)	1.01×10^{-28}
CO_2 (*gas*)	3.14×10^{-3}	CO_2 (*gas*)	1.27×10^{-3}
O_2 (*gas*)	1.52×10^{-3}	O_2 (*gas*)	6.36×10^{-4}
		I_2 (*gas*)	1.81×10^{-3}

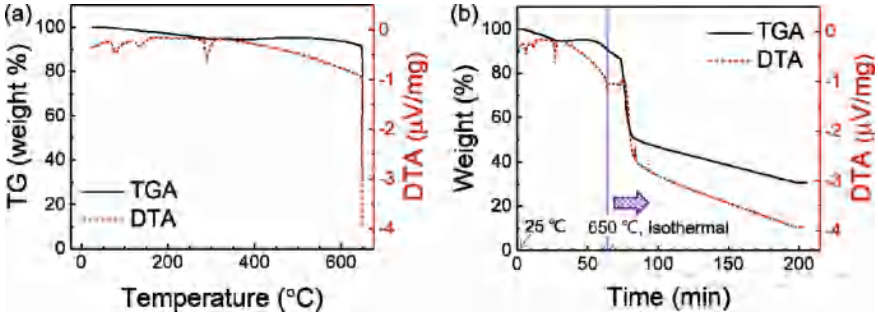

Fig. 3 – Results of thermalgravimetric analysis differential thermal analysis (TG-DTA) of $(Li_{0.62}K_{0.38})I$. condition: room temperature~650 °C (ramp. 10 °C/min) in nitrogen atmosphere and isothermal in CO_2: O_2 = 2:1 atm. (a) TG-DTA results by temperature dependence (b) TG-DTA results by time dependence.

electrolyte consumed by the lithiation process in the cathode during the early stages of operation was replenished via the injection of the electrolyte. However, contrary to expectation, we observed that the performance was negatively affected, if the electrolyte was injected continuously. At a current density of 150 mA/cm^2, the cell voltage was diminished by 26% and the IR increased by 62%. No nitrogen was detected at the anode effluent gas by GC analysis, which indicates that electrolyte loss is not the fatal cause of this degradation in performance.

This is an "electrolyte flooding" phenomenon [29] that occurs when an excessive amount of electrolyte presents in the MCFC unit cell, especially at the air electrode. Normally, the excess electrolyte charges the pores of both electrodes after filling all the pores of the matrix, in particular, the electrolyte is more soaked within the air electrode's pore due to its good wettability to the electrolyte [13,30–32]. Two methods which can be used to verify electrolyte flooding are electrochemical impedance spectroscopy (EIS) and O_2 gain. The Nyquist plot, obtained by EIS analysis, includes two overlapping semi-circles ranging from high frequency to low frequency [33].

Table 2 – Normal gas composition in a MCFC.

Temperature		650 °C
Sealing Pressure		2.0 kg_f/cm^2
Gas Utilization (U_f, U_o)		0.1 at 150 mA/cm^2
Gas Composition	fuel electrode	$H_2/CO_2/H_2O$ = 72:18:10
	air electrode	Air/CO_2 = 70:30
MCFC Components	fuel electrode	Ni-3wt%Al
	air electrode	*In-situ* lithiated NiO
	Matrix	γ - $LiAlO_2$
	Electrolyte	$(Li_{0.62}K_{0.38})_2CO_3$

Table 3 – Summary of amount of Li/K carbonate electrolyte injected until electrolyte flooding occurs at the cathode.

electrolyte	electrolyte injection No.						
	1	2	3	4	5	6	7
	injected electrolyte amount (g)						
Li_2CO_3	0.029	0.021	0.024	0.025	0.025	0.030	0.025
K_2CO_3	0.031	0.022	0.026	0.027	0.027	0.032	0.027
Total	0.060	0.043	0.050	0.052	0.052	0.062	0.051

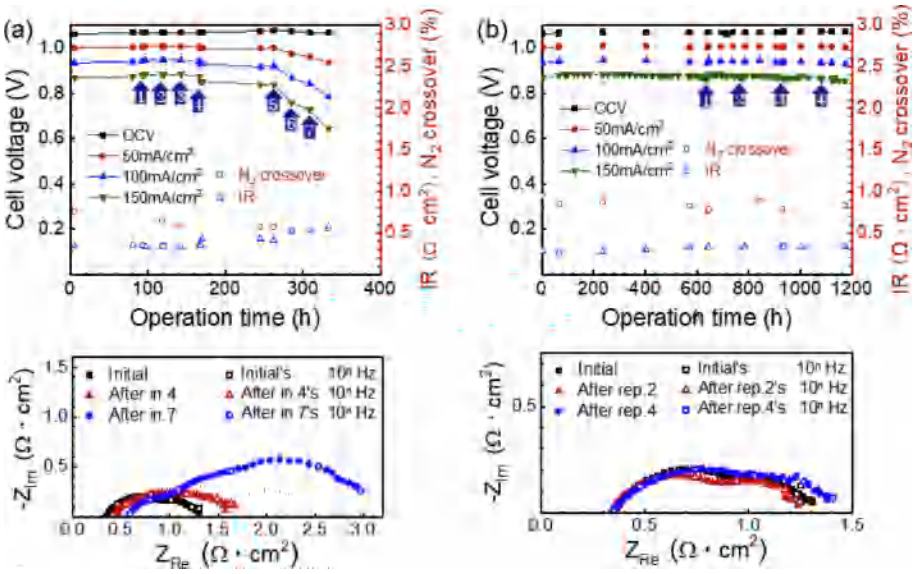

Fig. 4 – Results of the cell performance, nitrogen crossover, and electrochemical impedance spectroscopy (EIS) spectra. (a) electrolyte injection until electrolyte flooding occurs at the cathode. (b) long - term cell operation with an adequate amount of electrolyte replenishment.

The x-axis intercept in the Nyquist plot represents the ohmic resistance (R_{ohm}), which reflects the ionic conductivity of the electrolyte. The arc at the high frequency reflects the charge-transfer resistance (R_{CT}) and the other arc at the low frequency represents the mass-transfer resistance (R_{MT}) including the electrode resistances of gas solution & diffusion through the electrolyte film and gas-phase diffusion through the pores of the cathode. When an excess of electrolyte is present, a thick electrolyte film forms at the air electrode, increasing the diffusion distance for the O_2/CO_2 to the electrochemical reaction, thereby adversely affecting cell performance. The Nyquist plot in Fig. 4(a) shows that after 7 injections of the electrolyte, the semicircle in the low-frequency range corresponding to the R_{MT} in the Nyquist plot has become significantly larger.

Comparing impedance spectra of a standard cell with a flooding cell by using pure 'oxygen' instead of 'air' as the oxidant gas, the 'flooding cell' shows abnormally large impedance arc of R_{MT} due to high gas-phase diffusion resistance and high solution and diffusion resistance through the 'flooding' electrode [28,34]. In a standard cell, the performance difference, the so-called 'oxygen gain' value measured by the above method is about 80 mV at a current density of 150 mA/cm^2. However, in a cell where the cathode is filled with excessive electrolyte, the oxygen gain is more than 80 mV [10,35]. Therefore, it is possible to determine whether the cell is 'flooding' by comparing the 'oxygen gain' value [29,36]. As predicted, the values of oxygen gain after the 5th, 6th, and 7th electrolyte injections increased gradually to 82, 87, and 90 mV, respectively.

A comprehensive analysis of the experiments suggested that the excess electrolyte injected formed a thick film on the air electrode or plugged the pores of the electrode, and the performance decreased due to an increase in the R_{MT}.

Long-term operation of an MCFC unit cell with electrolyte replenishment

In order to limit electrolyte loss via vaporization during long-term operation, a 30 μm layer of corrosion-resistant Au was applied to the cell frame wet seal area, minimizing the loss of electrolytes due to corrosion.

The amount of electrolyte replenished during long-term operation is summarized in Table 4 and results from the analysis of performance, N_2 cross-over, and impedance are summarized in Fig. 4 (b). It was observed that during operations, a minor degradation in the performance is observed between 100 h and 642 h. The first replenishment of electrolyte was carried out at 652 h, and at this time there was a decrease in performance of 1.36% (0.875 V, based on the current density of 150 mA/·cm^2) and an increase in IR of approximately 25% (0.342 Ω·cm^2) as compared to the reference time at 101 h when the performance was 0,885 V (current density of 150 mA/cm^2) and the IR was 0.273 Ω·cm^2.

This means that through the replenishment of electrolyte, an IR decrease of about 3.2% (0.342 Ω·cm^2) and a performance increase of 1% (0.885 V, based on the current density of 150 mA/cm^2) was observed. It is assumed that the

Table 4 – Summary of the amount of Li/K carbonate electrolyte replenished in a unit cell during long-term operation.

electrolyte	electrolyte replenishment No.			
	1	2	3	4
	replenished electrolyte amount (g)			
Li_2CO_3	0.055	0.057	0.050	0.033
K_2CO_3	0.059	0.061	0.054	0.036
Total	0.114	0.118	0.104	0.069

performance did not fully recover due to the change in the composition of the electrolyte and the structural change of the components, among other factors, as the replenishment took place after the appropriate time for electrolyte replenishment had elapsed during long-term operation.

The second, third, and fourth replacement of the electrolytes proceeded at 787, 929, and 1079 h, respectively. The refill of the electrolyte decreased the IR by 6.9, 6.8, and 5.1%, respectively and no noticeable difference in performance was observed.

From the Nyquist plot in Fig. 4(b), it is clear that IR did not change significantly throughout the long-term operation and electrolyte replenishment. However, it was confirmed that either R_{CT} or R_{MT} was increased slightly under continuous injection. This is the result of injecting the electrolyte a little more than the consumed amount. The electrolyte injection should be performed before the hot spot is formed due to the lack of electrolyte in the matrix, and the electrolyte should be injected only before the 'flooding' state in which the electrolyte is excessively present in the electrode. This means that the cell or stack can be operated reliably for long-term operation of MCFC by injecting the appropriate amount of electrolyte at the right time.

According to Della Pietra et al. [24], the experiments proposed in this paper confirmed that the adequate injection timing for electrolyte injection was when the IR had increased by 10% compared to the reference value.

Electrolyte replenishment using electrolyte precursors (EPs) into unit cells

Injection of excess electrolyte precursors

The results of the above experiment showed that the unit cell is adversely affected when an excess electrolyte is injected, and in particular that the R_{MT} increased at the air electrode. In order to verify the adequacy of the selected EPs through thermodynamic calculations, after suitable pre-treatment process replenishment with the EPs was carried out in a stable unit cell for 100 h in a normal gas atmosphere. The amount of EP injected and converted to the electrolyte is shown in Table 5. Performance, IR, and N_2 cross-over analysis results during the operation of the MCFC unit cell at the anode outlet are summarized in Fig. 5(a). During the operation of the unit cell, it was confirmed that the N_2 cross-over was maintained at less than 1% during the EP injection, and there is a slight decrease in performance after the first EP injection, but this can be regarded as within the range of acceptable error.

Increasing the number of injection (e.g. eight), the cell voltage drastically decreased to 0.508 V at the current density of 150 mA/cm^2 due to the excess of electrolytes. However, after the final EP refill, no additional changes in N_2 cross-over or IR were detected. In the Nyquist plot, a continuous increase in R_{CT} and R_{MT} was observed as the injection of EP continued, and after the 8th addition, the R_{MT} increased drastically from 1.452 Ω·cm^2 to 2.737 Ω·cm^2 (Fig. 5(a)). This phenomenon is due to the formation of a thick electrolyte film produced by the injected EP in the air electrode, resulting in an increase of mass-transfer resistance, R_{MT}, at the cathode. This result is similar to previous experiments surrounding the excessive injection of electrolyte, and through the experiment, we were able to identify that LiI and KI, which were injected as EP, served as adequate substances for replacement of electrolyte.

Long-term operation of a unit cell with electrolyte precursors replenishment

As described in section Electrolyte replenishment using electrolyte precursors (EPs) into unit cells, 30 μm of Au was coated on the wet seal area, minimizing the corrosion arising from the presence of electrolytes. The EP, $(Li_{0.62}K_{0.38})I$, which was prepared in advance, was replenished and long-term operation of the MCFC unit cell proceeded (the amount injected at each replenishment is summarized in Table 6). Results of the performance and EIS analysis for each injection are summarized in Fig. 5(b). The maximum performance was observed in 218 h after the pre-treatment, with 0.875 V (current density 150 mA/cm^2) and IR 0.271 Ω·cm^2. Continuous degradation of performance in the unit cell was observed after 220 h of operating. Due to the large molecular weight of the prepared EP, the amount of injected EP was quantitatively greater than the electrolyte. Through the replenishment with an adequate amount of EP by 6 times, we were able to confirm a temporary improvement in performance, and we observed that the MCFC operated stably for 886 h.

After the 7th replenishment of EP, the unit cell was operated at a current density of 150 mA/㎠without any replenishment during 164 h. In this time, a rapid degradation in performance was observed. Also, the OCV fell drastically to 0.736 V and N_2 cross-over identified at the anode effluent was 23.8%. From this result, we can assume that neither fuel gas nor air gas can maintain the partial pressure inside the cell,

Table 5 – Summary of amount of electrolyte precursors (LiI and KI) injected until electrolyte flooding occurs at the cathode.

EP	EP injection No.							
	1	2	3	4	5	6	7	8
	injected EP amount (g)							
LiI	0.05	0.086	0.077	0.108	0.091	0.118	0.114	0.517
KI	0.038	0.066	0.059	0.082	0.069	0.09	0.087	0.393
electrolyte	converted amount of electrolyte (g)							
Li_2CO_3	0.013	0.023	0.021	0.029	0.025	0.032	0.031	0.142
K_2CO_3	0.015	0.027	0.024	0.034	0.028	0.037	0.036	0.163
Total	0.029	0.051	0.045	0.063	0.053	0.070	0.067	0.306

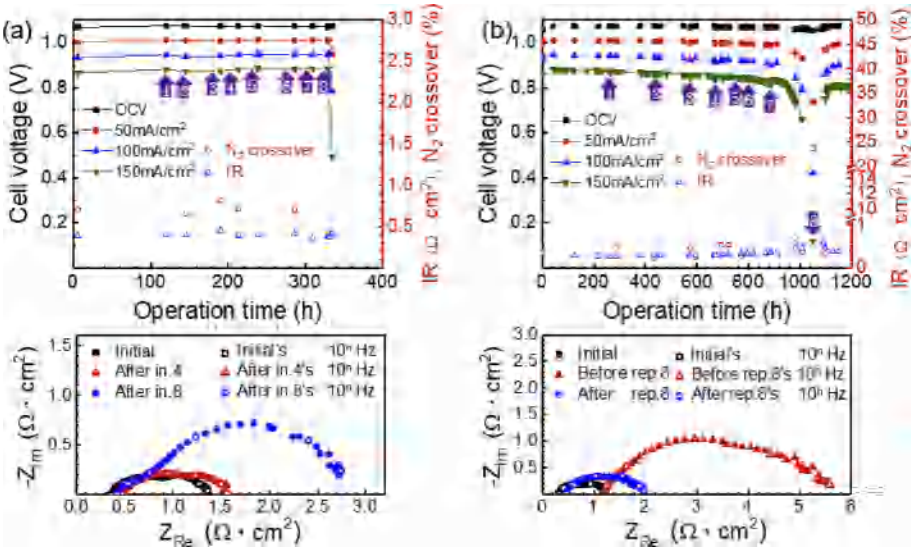

Fig. 5 – Results of the cell performance, nitrogen crossover, and EIS spectra. (a) electrolyte precursor injection until electrolyte flooding occurs at the cathode. (b) Electrolyte precursor injections after induction of electrolyte consumption through an accelerated operation.

Table 6 – Summary of the amount of electrolyte precursors (LiI and KI) replenished in a unit cell during long-term operation.

EP	EP replenishment No.							
	1	2	3	4	5	6	7	8
	replenished EP amount (g)							
LiI	0.087	0.062	0.065	0.063	0.050	0.027	0.068	0.190
KI	0.066	0.047	0.049	0.048	0.038	0.021	0.051	0.144
Electrolyte	converted amount of electrolyte (g)							
Li_2CO_3	0.024	0.017	0.017	0.017	0.013	0.007	0.018	0.052
K_2CO_3	0.027	0.019	0.020	0.019	0.015	0.008	0.021	0.059
Total	0.051	0.036	0.038	0.037	0.029	0.016	0.039	0.112

and burning occurred due to direct contact between the O_2 and the H_2. It could lead to the excessive consumption of electrolyte via corrosion or vaporization due to the suddenly soaring temperature. Therefore, the EIS analysis showed that the IR increased to 1.13 Ω · ㎠ and the overall impedance spectra shifted to the right significantly (shown in Fig. 4(b), "before rep. 8").

However, since the 8th replenishment of EP, the OCV and N_2 cross-over returned to the level of operation at 920 h. The IR also decreased by 66.4% to 0.38 Ω · ㎠, returning to the standard level of an MCFC unit cell, and R_{CT} and R_{MT} also recovered to a certain extent but were not fully restored to the levels at the initial state of operation (Fig. 4(b), "after rep. 8"). It is assumed that this phenomenon is a result of a huge change in the composition of the electrolytes within the cell and that the micropore structure of the electrode was destroyed due to the hot spot.

This phenomenon verified that the restoration of performance using electrolyte replenishment was possible in the "phase 2, rapid degradation" section in Fig. 1, and that at the same time, electrolyte replenishment of MCFCs and long-term operation were made possible by using EPs.

Table 7 – Summarization of performance with electrolyte or electrolyte precursor injected unit cells.

injection No.	electrolyte injected cell				EP injected cell			
	operating time (h)	injected electrolyte (g)	IR (Ω x cm^2)	voltage at 150 mA/cm^2 (V)	operating time (h)	injected EP (converted) (g)	IR (Ω x cm^2)	voltage at 150 mA/cm^2 (V)
1	92	0.060	0.355	0.880	120	0.029	0.401	0.881
2	118	0.043	0.342	0.883	143	0.051	0.397	0.878
3	142	0.050	0.3313	0.884	179	0.045	0.454	0.875
4	166	0.052	0.353	0.874	211	0.063	0.386	0.880

In conclusion, according to the 3.2.1 and 3.3.1 experimental results, the EP injection to a unit cell has similar positive effects on performance or polarization degradation mitigation by the Li/K carbonate electrolyte injection (Table 7). However, an excess amount of EP injected to a unit cell showed adverse effects just like electrolyte over-injected cell. Therefore, long-term operation of MCFC is expected to be possible through an adequate amount of EP supplementation.

Conclusion

This study explores and verifies the possibility of EPs which can be injected the electrolyte as a liquid or gas phase into an MCFC unit cell so that the electrolyte can be supplemented in a homogeneous concentration for the long-term operation of an MCFC stack. The in-situ EPs (LiI, KI) replenishment into MCFC unit cell showed a similar tendency with the $(Li/K)_2CO_3$ electrolyte replenishment. When the electrolyte was replenished by adequate amounts, the performance and impedance were restored but the R_{MT} increased and the following degradation in performance was identified at the time of over-injection (Pore filling ratio [36], "PFR = (impregnated electrolyte volume in cell)/(total pore volume [air, fuel electrode and matrices])". State-of the art MCFCs has PFR 70–80%. In this study, PFR >88%). Furthermore, we have succeeded in attaining over 1000 h operation of MCFC unit cell under the severe operating conditions through in-situ EPs replenishment. In particular, when the EPs were replenished where there was a significant loss of electrolytes leading to drastic performance degradation as in degradation phase 2, it was identified that the cell performance and the impedance resistances recovered to the normal degradation range.

In conclusion, this study identified that LiI and KI are adequate for use as EPs for replenishing the electrolyte consumed during the long-term operation of MCFCs. Favourable EPs, LiI and KI, have a low melting point and high vapor pressure so that they are capable to replenish the electrolyte of MCFC as liquid or gas phase. In other words, it means that LiI and KI have the feasibility of electrolyte replenishment as a liquid phase at the low temperature of below 300 °C and as a gas phase at the operating temperature (650 °C) of MCFC. It is expected that future studies into the replenishment of MCFC stacks will enable the long-term operation of 40,000 h or more when an adequate amount of EPs is replenished as a liquid or gas phase.

Acknowledgements

This work was financially supported by the Energy Technology Program of Korea Institute of Energy Technology Evaluation and Planning (KETEP) (20163030031860) and the Ministry of Trade, Industry & Energy (MOTIE) of Korea and the Creative Materials Discovery Program by Ministry of Science and ICT (2018M3D1A1058536) and the KIST institutional program for the Korea Institute of Science and Technology (2E29610).

REFERENCES

[1] Yuh C, Johnsen R, Farooque M, Maru H. Status of carbonate fuel cell materials. J Power Sources 1995;56:1–10. https://doi.org/10.1016/0378-7753(95)80001-W.
[2] Selman JR. Molten-salt fuel cells—technical and economic challenges. J Power Sources 2006;160:852–7. https://doi.org/10.1016/j.jpowsour.2006.04.126.
[3] O'Hayre R, Cha S-W, Colella W, Prinz FB. Fuel cell fundamentals. Hoboken, NJ, USA: John Wiley & Sons, Inc; 2016. https://doi.org/10.1002/9781119191766.
[4] W V, HA G, H Y. Handbook of fuel cells: advances in electrocatalysis, materials. Diagnostics; 2009.
[5] Larminie J, Dicks A. Fuel cell systems explained. West Sussex, England: John Wiley & Sons, Ltd; 2003. https://doi.org/10.1002/9781118878330.
[6] Nguyen QM. Technological status of nickel oxide cathodes in molten carbonate fuel cells — a review. J Power Sources 1988;24:1–19. https://doi.org/10.1016/0378-7753(88)80085-5.
[7] Duan L, Sun S, Yue L, Qu W, Yang Y. Study on a new IGCC (integrated gasification combined cycle) system with CO2 capture by integrating MCFC (molten carbonate fuel cell). Energy 2015;87:490–503. https://doi.org/10.1016/j.energy.2015.05.011.
[8] Dimopoulos GG, Stefanatos IC, Kakalis NMP. Exergy analysis and optimisation of a marine molten carbonate fuel cell system in simple and combined cycle configuration. Energy Convers Manag 2016;107:10–21. https://doi.org/10.1016/j.enconman.2015.09.007.
[9] Zhang H, Chen B, Xu H, Ni M. Thermodynamic assessment of an integrated molten carbonate fuel cell and absorption refrigerator hybrid system for combined power and cooling applications. Int J Refrig 2016;70:1–12. https://doi.org/10.1016/j.ijrefrig.2016.07.011.
[10] Milewski J, Discepoli G, Desideri U. Modeling the performance of MCFC for various fuel and oxidant compositions. Int J Hydrogen Energy 2014;39:11713–21. https://doi.org/10.1016/j.ijhydene.2014.05.151.
[11] Accardo G, Frattini D, Moreno A, Yoon SP, Han JH, Nam SW. Influence of nano zirconia on NiAl anodes for molten carbonate fuel cell: characterization, cell tests and post-analysis. J Power Sources 2017. https://doi.org/10.1016/j.jpowsour.2016.11.029.
[12] Frattini D, Accardo G, Moreno A, Yoon SP, Han JH, Nam SW. A novel Nickel-Aluminum alloy with Titanium for improved anode performance and properties in Molten Carbonate Fuel Cells. J Power Sources 2017;352:90–8. https://doi.org/10.1016/j.jpowsour.2017.03.112.
[13] Lee CG. Influence of temperature on the anode reaction in a molten carbonate fuel cell. J Electroanal Chem 2017;785:152–8. https://doi.org/10.1016/j.jelechem.2016.12.032.
[14] Morita H, Kawase M, Mugikura Y, Asano K. Degradation mechanism of molten carbonate fuel cell based on long-term performance: long-term operation by using bench-scale cell and post-test analysis of the cell. J Power Sources 2010;195:6988–96. https://doi.org/10.1016/j.jpowsour.2010.04.084.
[15] Huijsmans JP, Kraaij G, Makkus R, Rietveld G, Sitters E, Reijers HT. An analysis of endurance issues for MCFC. J Power Sources 2000;86:117–21. https://doi.org/10.1016/S0378-7753(99)00448-6.
[16] Lee M, Lee C-W, Ham H-C, Han J, Yoon SP, Lee KB. Mechanical strength improvement of aluminum foam-reinforced matrix for molten carbonate fuel cells. Int J Hydrogen Energy 2017;42:16235–43. https://doi.org/10.1016/j.ijhydene.2017.03.096.

[17] Frattini D, Accardo G, Moreno A, Yoon SP, Han JH, Nam SW. Strengthening mechanism and electrochemical characterization of ZrO_2 nanoparticles in nickel-aluminum alloy for molten carbonate fuel cells. J Ind Eng Chem 2017. https://doi.org/10.1016/j.jiec.2017.07.021.
[18] Donado RA. Corrosion of the wet-seal area in molten carbonate fuel cells. J Electrochem Soc 1984;131:2535. https://doi.org/10.1149/1.2115354.
[19] Frangini S. Corrosion of metallic stack components in molten carbonates: critical issues and recent findings. J Power Sources 2008;182:462–8. https://doi.org/10.1016/j.jpowsour.2007.11.100.
[20] Bergman B, Lagergren C, Lindbergh G, Schwartz S, Zhu B. Contact corrosion resistance between the cathode and current collector plate in the molten carbonate fuel cell. J Electrochem Soc 2001;148:A38. https://doi.org/10.1149/1.1339027.
[21] Zhu B, Lindbergh G, Simonsson D. Comparison of electrochemical and surface characterisation methods for investigation of corrosion of bipolar plate materials in molten carbonate fuel cell. Corros Sci 1999;41:1497–513. https://doi.org/10.1016/S0010-938X(98)00200-5.
[22] Y SP, H IO, Han JH, Nam SW, J SC, Song SA. Molten carbonate fuel cells including reinforced lithium aluminate matrix, method for preparing the same, and method for supplying lithium source. 2015.
[23] Sugiura K, Yamauchi M, Tanimoto K, Yoshitani Y. Evaluation of volatile behaviour and the volatilization volume of molten salt in DIR-MCFC by using the image measurement technique. J Power Sources 2005;145:199–205. https://doi.org/10.1016/j.jpowsour.2004.12.079.
[24] Della Pietra M, McPhail SJ, Prabhakar S, Desideri U, Nam SW, Cigolotti V. Accelerated test for MCFC button cells: first findings. Int J Hydrogen Energy 2016;41:18807–14. https://doi.org/10.1016/j.ijhydene.2016.07.021.
[25] Kojima T, Miyazaki Y, Nomura K, Tanimoto K. Density, surface tension, and electrical conductivity of ternary molten carbonate system Li2CO3–Na2CO3–K2CO3 and methods for their estimation. J Electrochem Soc 2008;155:F150. https://doi.org/10.1149/1.2917212.
[26] Kojima T, Miyazaki Y, Nomura K, Tanimoto K. Density, molar volume, and surface tension of molten Li2CO3-Na2CO3 and Li2CO3-K2CO3 containing alkaline earth (Ca, Sr, and Ba) carbonates. J Electrochem Soc 2003;150:E535. https://doi.org/10.1149/1.1611494.
[27] Stanford University., & Reynolds WC. STANJAN: interactive computer programs for chemical equilibrium analysis. 1981.
[28] Kulkarni A, Giddey S. Materials issues and recent developments in molten carbonate fuel cells. J Solid State Electrochem 2012;16:3123–46. https://doi.org/10.1007/s10008-012-1771-y.
[29] K S-G, SP Y, H J, SW N, L T-H, H S-A. A stabilized NiO cathode prepared by sol-impregnation of LiCoO2 precursors for molten carbonate fuel cells. J Power Sources 2002;112:109–15. https://doi.org/10.1016/S0378-7753(02)00358-0.
[30] Kim YJ, Kim TK, Lee SW, Lee KJ, Lee CG. Effect of electrolyte amount on the performance in a molten carbonate fuel cell. In: Meeting abstracts. Meet abstr. Electrochem Soc; 2016. No 1, Pp 175-175.
[31] Youn JY, Yoon SP, Han J, Nam SW, Lim T-H, Hong S-A, et al. Fabrication and characteristics of anode as an electrolyte reservoir for molten carbonate fuel cell. J Power Sources 2006;157:121–7. https://doi.org/10.1016/j.jpowsour.2005.07.068.
[32] Accardo G, Frattini D, Yoon SP, Ham HC, Nam SW. Performance and properties of anodes reinforced with metal oxide nanoparticles for molten carbonate fuel cells. J Power Sources 2017. https://doi.org/10.1016/j.jpowsour.2017.10.015.
[33] Lee C. Analysis of impedance in a molten carbonate fuel cell. J Electroanal Chem 2016;776:162–9. https://doi.org/10.1016/j.jelechem.2016.07.005.
[34] Audasso E, Bosio B, Nam S. Extension of an effective MCFC kinetic model to a wider range of operating conditions. Int J Hydrogen Energy 2016;41:5571–81. https://doi.org/10.1016/j.ijhydene.2015.10.152.
[35] Scaccia S, Frangini S. Oxygen dissolution behaviour in (52/48) mol% Li2CO3/Na2CO3 electrolyte containing Ba and Ca additives. J Mol Liq 2006;129:133–7. https://doi.org/10.1016/j.molliq.2006.02.006.
[36] Kim Y-J, Kim T-K, Lee K-J, Lee C-G. Performance analysis with various amounts of electrolyte in a molten carbonate fuel cell. J Electrochem Sci Technol 2016;7:234–40. https://doi.org/10.5229/JECST.2016.7.3.234.